Optimization of Neutron Guide Geometry for the short-HIBEAM beamline at ESS

Axel Borg

August 2025

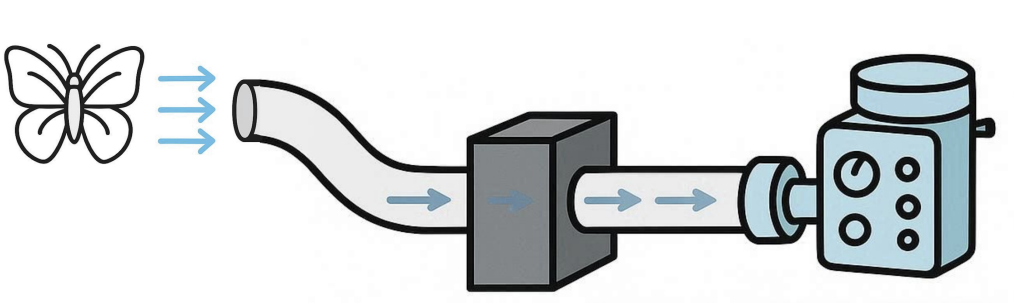

Abstract

This report presents an optimized design for neutron guides in the proposed short-HIBEAM beamline, analyzing key parameters such as guide angles, widening, supermirror m-values, and bender configurations. Monte Carlo simulations of neutron optics were conducted using the McStas software package. The results provide valuable insights into maximizing neutron intensity within a 30 cm target region, providing a foundation for informed design decisions for future particle physics experiments at ESS.

Supervisors:
Linus Persson
Matthias Holl

Group Leader:
Valentina Santoro

EUROPEAN SPALLATION SOURCE

LUND UNIVERSITY

Contents

1 Introduction

Science has always advanced by pushing the limits of our ability to probe the smallest scales of nature. From the discovery of the neutron a century ago to the present day, particle and nuclear physics have relied on increasingly powerful sources to provide the beams necessary for experiments. Neutrons are unique among probes because they are electrically neutral and deeply penetrating, which makes them particularly valuable in studies ranging from fundamental particle physics to materials science and energy research. The global scientific community has therefore invested heavily in building ever-brighter neutron sources to enable discoveries that cannot be achieved otherwise.

The European Spallation Source (ESS), currently under construction in Lund, Sweden, is designed to be the brightest neutron source in the world. Its primary mission is to provide unprecedented opportunities in materials science, chemistry, and biology, but it also holds great potential for particle and nuclear physics.

ESS will generate neutrons through proton bombardment of a rotating tungsten target. Powered by a 2 GeV proton accelerator, the collisions between protons and tungsten nuclei will produce a high flux of neutrons. These neutrons first pass through the moderator, which slows down the high-energy neutrons generated in the spallation process via repeated collisions with light nuclei. This shifts their energy spectrum from the fast (MeV) range to thermal or cold (meV) neutrons, making them more suitable for a wide array of experimental applications.

Following moderation, the neutrons are transported via a neutron guide system. These guides function like pipes for channeling low-energy neutrons, constructed with various materials and coatings to enhance reflectivity and often incorporating supermirrors. Supermirrors are highly polished, multilayered structures designed to efficiently reflect neutron beams. The first extraction guide is inserted in the steel shielding of the monolith and is a specialized, high-efficiency guide embedded that directs neutrons from the moderator assembly toward the beam ports. Beyond this, the neutrons proceed through additional neutron guides, each specially designed to meet the needs of specific experimental stations.

At present, ESS does not include a dedicated beamline for particle physics experiments. The HIBEAM collaboration seeks to address this by designing a versatile, multi-purpose beamline optimized for such research. A key challenge is understanding how different guide configurations affect neutron distribution and intensity in order to support design decisions. Experimental testing is not possible at this stage, making detailed Monte Carlo simulations essential.

A small but non-negligible portion of neutrons emitted from the ESS moderator are fast neutrons, which substantially increase the detector's overall count rate and the dose rate around the beamline while contributing minimally to experimental sensitivity. To mitigate this, neutron guides can incorporate benders, which intentionally break the line of sight between the source and the experimental area. Slower neutrons, having higher critical reflection angles, are more likely to follow the curved guide, whereas faster neutrons travel approximately straight and are absorbed by shielding. This approach reduces unwanted high-energy neutron flux in the target region while providing the desired spectrum for experiments.

The purpose of this internship was to perform neutron transport simulations using the McStas software package to evaluate and optimize beamline components for the proposed HIBEAM beamline. The work focused on characterizing the neutron distribution in a reference setup, exploring how variations in guide geometry, such as angles, widening and m-values, affect the intensity reaching an area as big as the detector intended for initial experiments, located 10 meters from the guide exit. Furthermore, bender designs were investigated to assess their impact on intensity and wavelength spectrum, aiming to identify configurations that balance shielding requirements with flux performance.

2 Method & Results

Simulations were conducted in McStas version 3.5.32 to optimize neutron guide designs by maximizing the intensity reaching a detector located 10 m downstream of the guide exit, expected to be similar to a circular region with 30 cm diameter. The workflow combined scripted parameter sweeps, automated post-processing and uncertainty propagation to compare straight guides and bender configurations on equal footing.

Neutrons were sourced using the "ESS_butterfly" component, configured with sector = "E" and beamline = 5. The "monolith insert" served as the neutron extraction guide for all simulations. A minimum of 10^6 neutrons were simulated in each case, with selected simulations using 10^7 neutrons as noted in the text. Wavelength spectra were measured using the Monitor_nD component, placed directly after the guide exit. Neutron distributions was collected by a PSD_monitor, always 10 meters after the guide exit.

Each simulation was launched by a Bash script that recorded the parameter set together with data collected from every monitor. From the PSD_monitor, distribution data and standard deviations were placed into two matrices. Post-processing in Python integrated the intensity over a movable circular mask of 30 cm diameter by inferring bin dimensions from the parameter set to construct the mask and applying `scipy.ndimage.convolve` to produce a matrix of integrated intensities. The position yielding the maximum integrated intensity was identified using the function `numpy.unravel_index`. The statistical uncertainty within the optimal mask was propagated as

$$\sigma = \sqrt{\sum_{\Omega} \sigma_{\text{bin}}^2}, \tag{1}$$

where Ω denotes all bins inside the mask and σ_{bin} the per-bin standard deviation.

2.1 Angle Variation

The angle study was performed using the McStas simulation layout depicted in Figure 1. The coordinate system follows the BPCS (beam port coordinate system), with the y-axis aligned vertically and the x- and z-axes spanning the horizontal plane (z along the beam direction). A straight neutron guide, with a rectangular cross section of $0.182 \times 0.152\ m^2$, was rotated independently around the x-axis (θ_x) and y-axis (θ_y) relative the z-axis. For each rotation angle, the intensity was calculated within the circular area positioned at 25 m. The resulting intensity map is presented in 2a and 2b as heatmaps to locate the optimum. The optimal angle was found to be approximately $\theta_x = 0.33°$ and $\theta_y = -0.28°$.

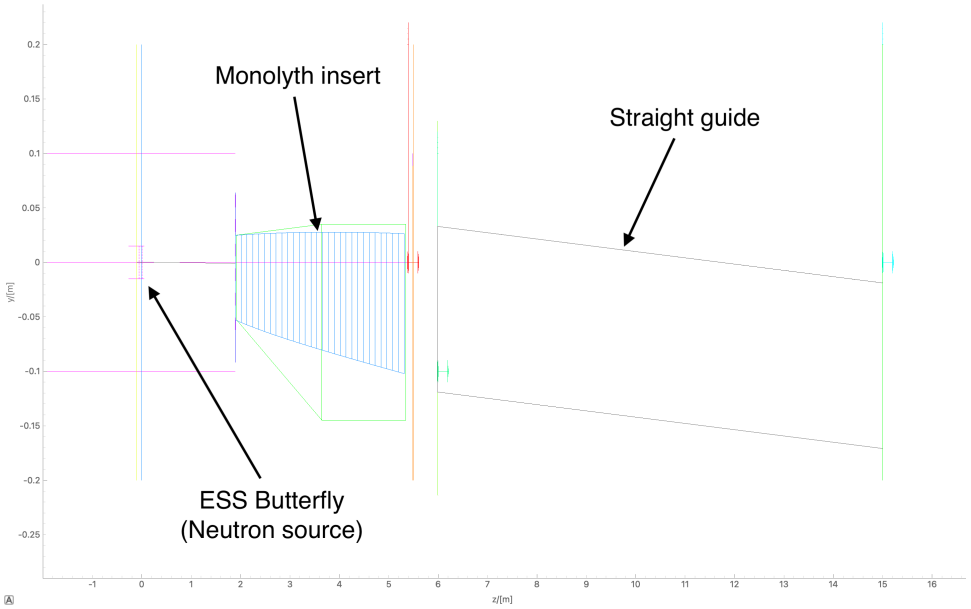

Figure 1: McStas setup: angle: $\theta_x = 0.33°$, $\theta_y = -0.28°$

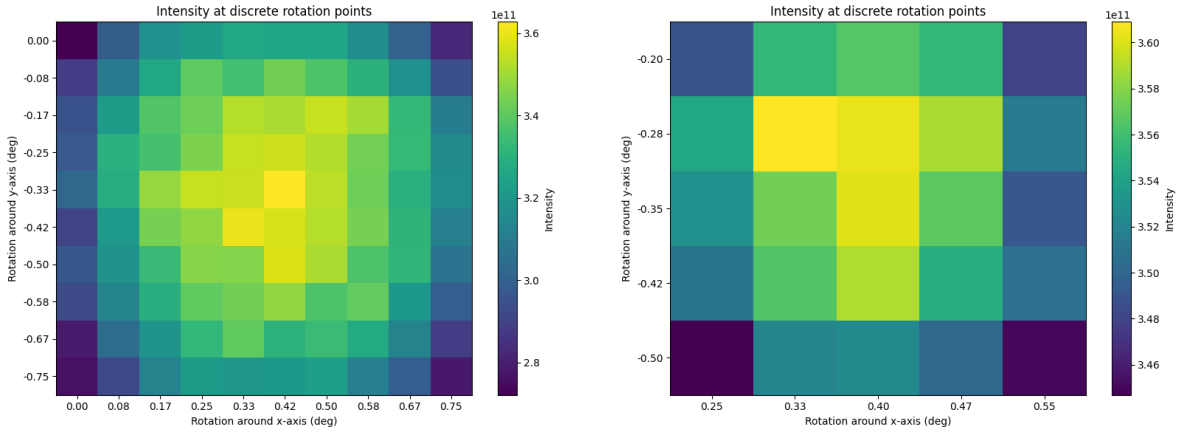

(a) Rotation around x-axis from 0° to 0.75° and y-axis from −0.75° to 0°, simulating 10^6 neutrons per data point

(b) Rotation around x-axis from 0.25° to 0.55° and y-axis from −0.20° to −0.50°, simulating 10^7 neutrons per data point

Figure 2: Heatmaps of intensity in a 30 cm diameter circular area located 10 m downstream from a straight neutron guide, as a function of rotation around x and y axis (in degrees)

2.2 Widening Variation

Neutron intensity was examined using the configuration shown in Figure 3, where a neutron guide, with a fixed cross section of 0.182 × 0.152 m^2 at its entrance, was linearly widened to the detector side to optimize intensity. Keeping the angles fixed at the best values from the previous subsection ($\theta_x = 0.33°$, $\theta_y = -0.28°$), the sides of the opening was scaled by a widening factor and its impact on intensity at 10 m is shown in Figure 4a and for a narrower range in Figure 4b. A factor of 7.4% increase in intensity as compared to a completely rectangular guide, was found at widening factor 1.237, widening from 0.182 × 0.152 m^2 at the entrance to 0.225 × 0.188 m^2 at the exit. Above this widening factor, the intensity decreases and comes to a plateau at the value you get without a guide.

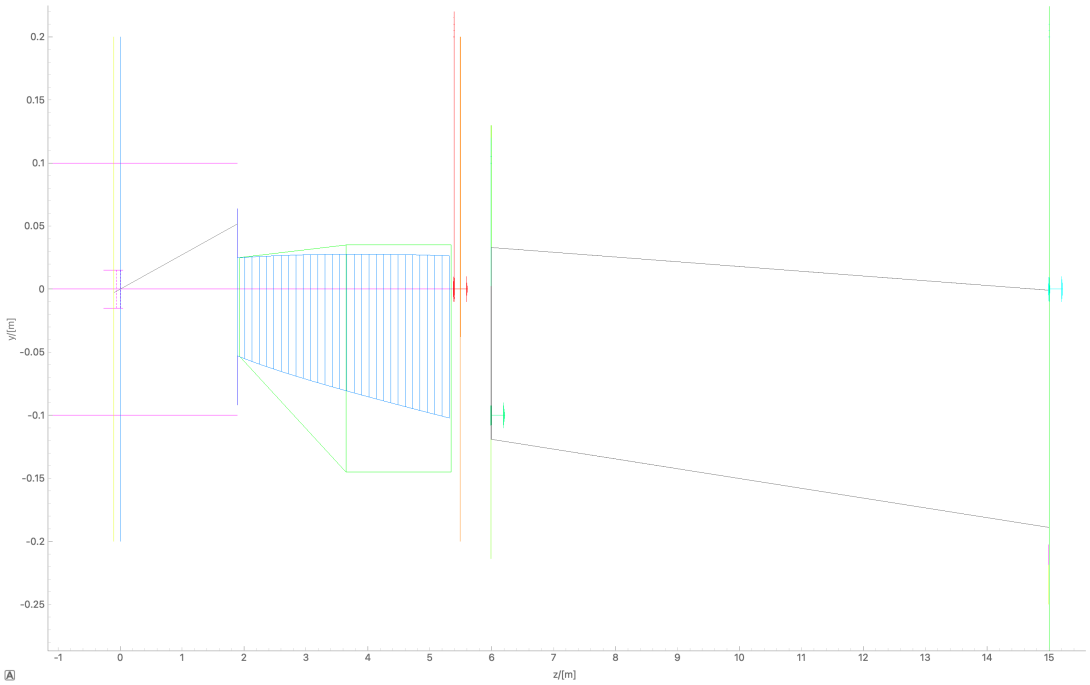

Figure 3: McStas setup: angle: $\theta_x = 0.33°$, $\theta_y = -0.28°$, widening factor = 1.237

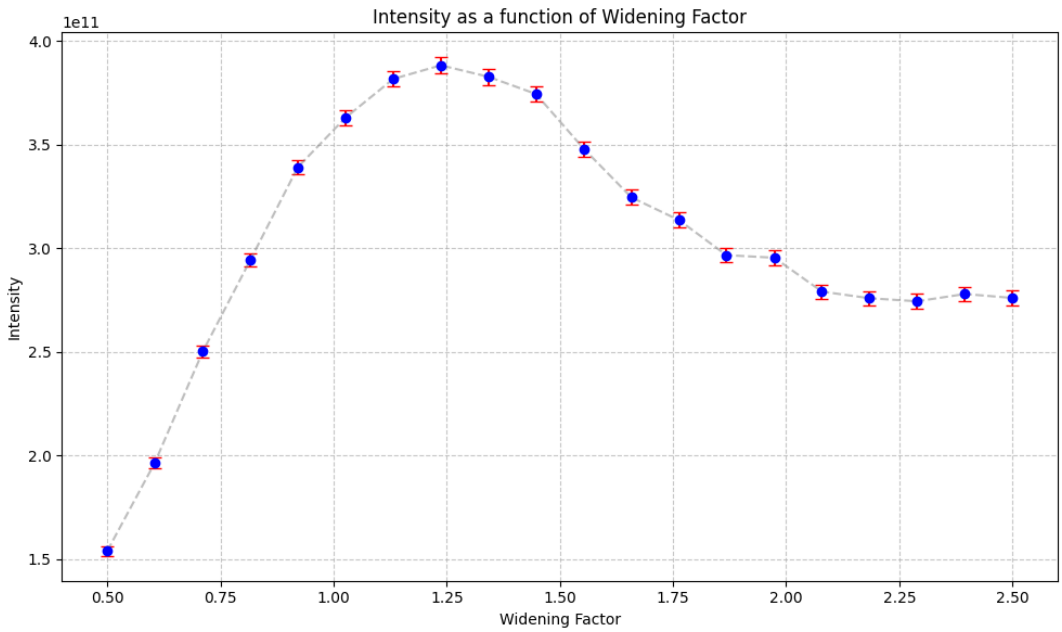

(a) Widening of guide opening [0.5,2.5], simulating 10^6 neutrons per data point

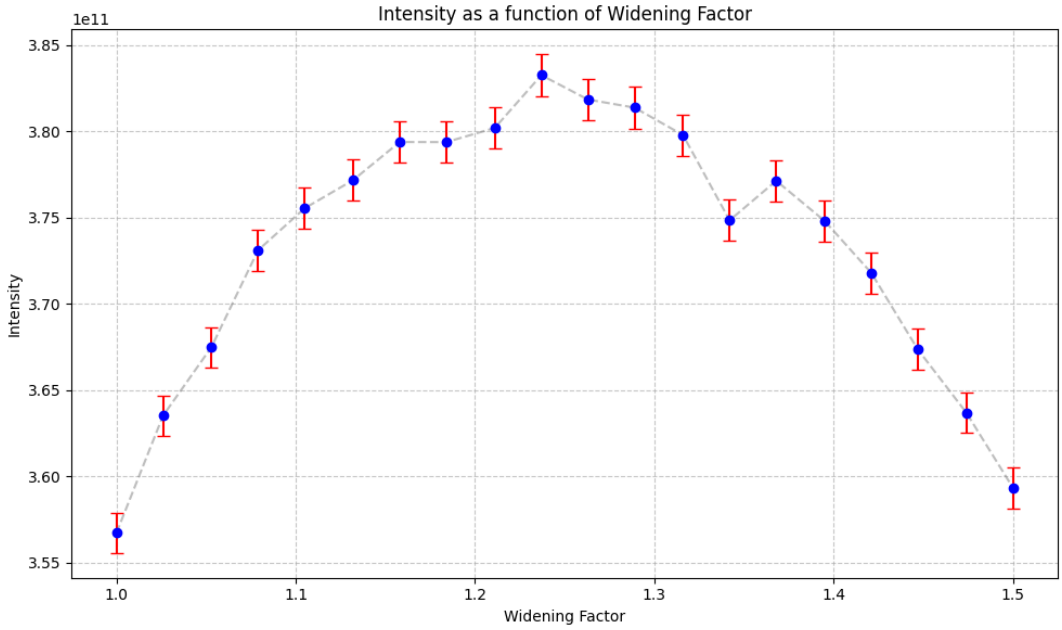

(b) Widening of guide opening [1,1.5], simulating 10^7 neutrons per data point

Figure 4: Plots of intensity in a 30 cm diameter circular area located 10 m downstream from a neutron guide rotated $\theta_x = 0.33°$, $\theta_y = -0.28°$, as a function of widening the opening on the detector side.

2.3 m-Value Variation

With angle and widening fixed (angle $\theta_x = 0.33°$, $\theta_y = -0.28°$; widening factor = 1.237), the supermirror m-value was varied while holding all other geometry constant to isolate reflectivity effects on the integrated intensity and the wavelength spectrum directly after the guide. Figure 5a shows the intensity, and Figure 5b shows the wavelength distribution immediately after the straight guide with m-value = 1.

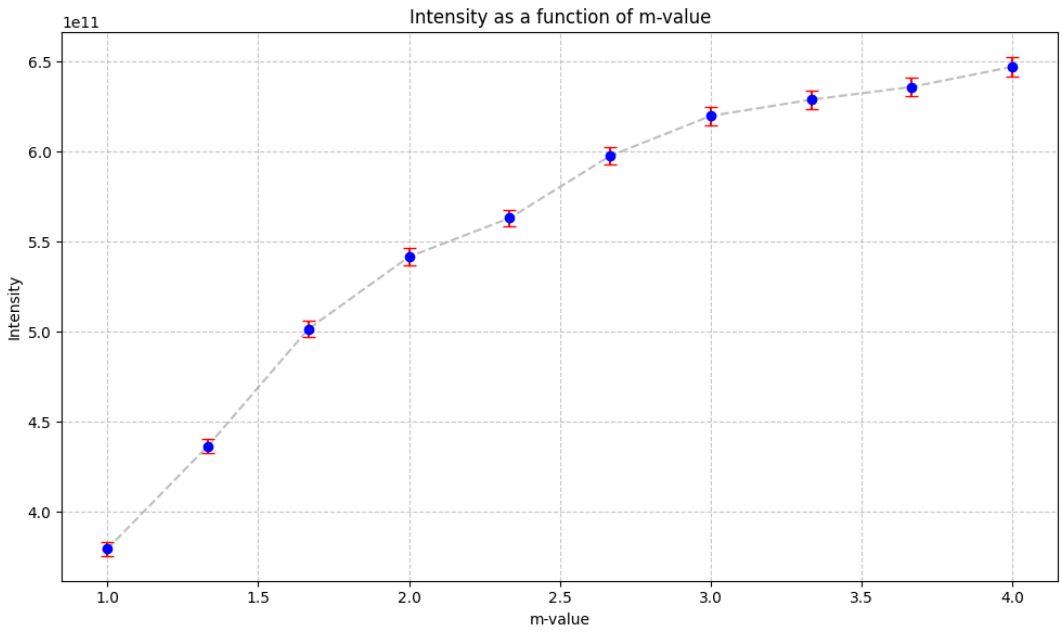

(a) Intensity as a function of m-value

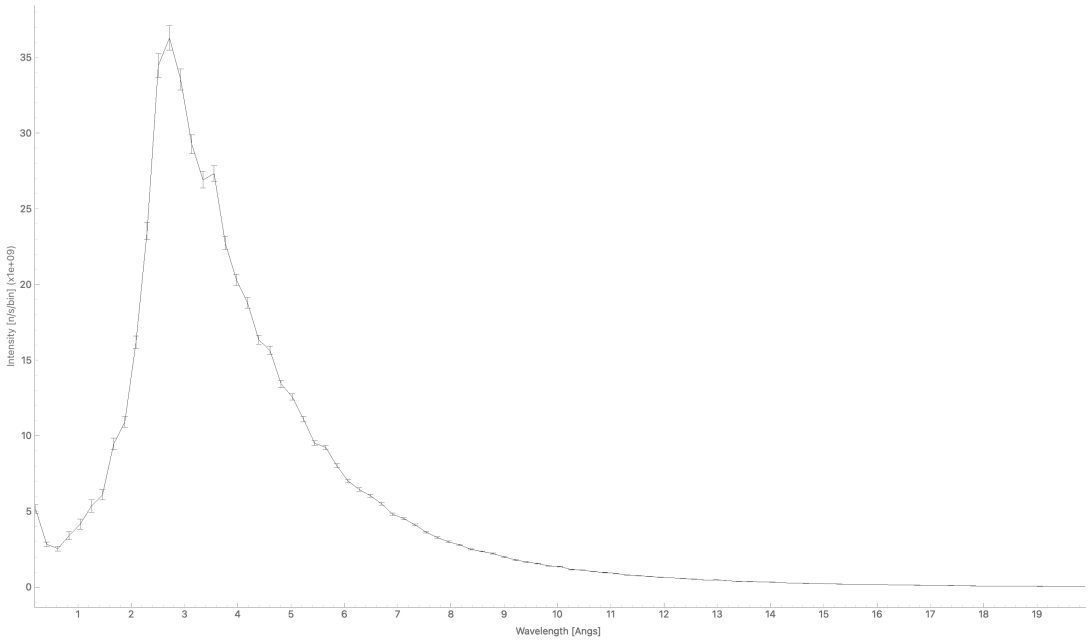

(b) Wavelength spectrum right after straight guide

Figure 5: Intensity and wavelength spectrum for straight guide, angle: $\theta_x = 0.33°$, $\theta_y = -0.28°$, widening factor = 1.237

2.4 Bender Analysis and Simplification

Bender performance was studied, starting from the nEDM model in Figure 6. The nEDM model breaks line of sight twice and has 12 slits, which means that the guide is horizontally separated into 12 different thinner guides that run alongside each other.

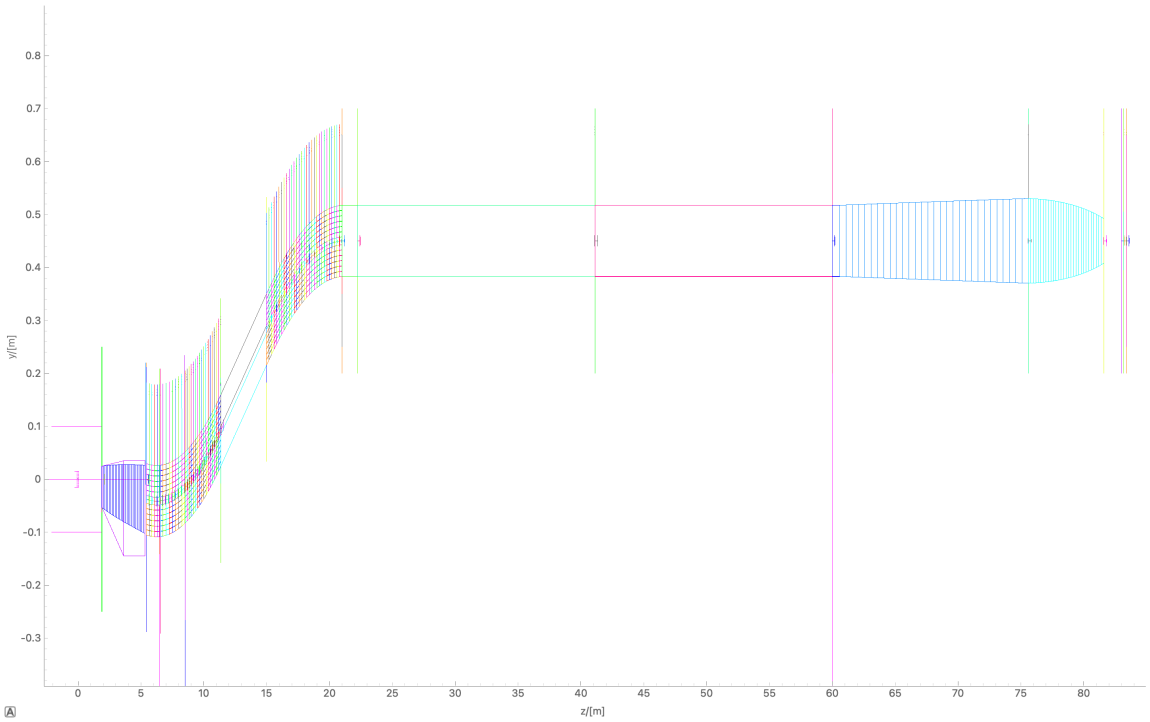

Figure 6: Original nEDM McStas model used as the baseline for bender studies.

Components downstream of the bending guides were removed and the bender was simplified by unifying the guide elements. A monitor was placed immediately after the bender to capture wavelength and another at 10 m downstream from the bender exit to capture intensity. Two simplified layouts were constructed where line of sight is lost once and twice, respectively, as illustrated in Figures 7a and 7b. In Figure 8, intensity is plotted as a function of the number of slits and in Figure 9 the resulting wavelength distributions are shown.

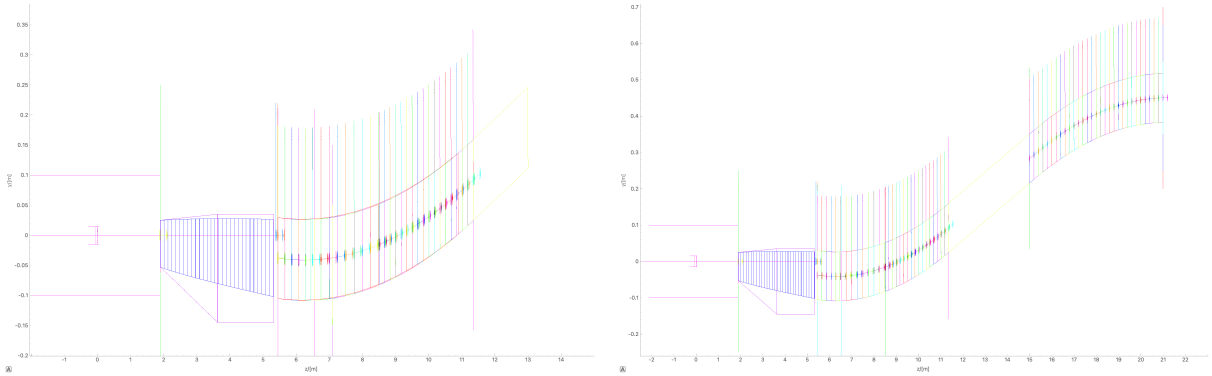

(a) McStas setup: Losing line of sight once

(b) McStas setup: Losing line of sight twice

Figure 7: Simplifications of nEDM model

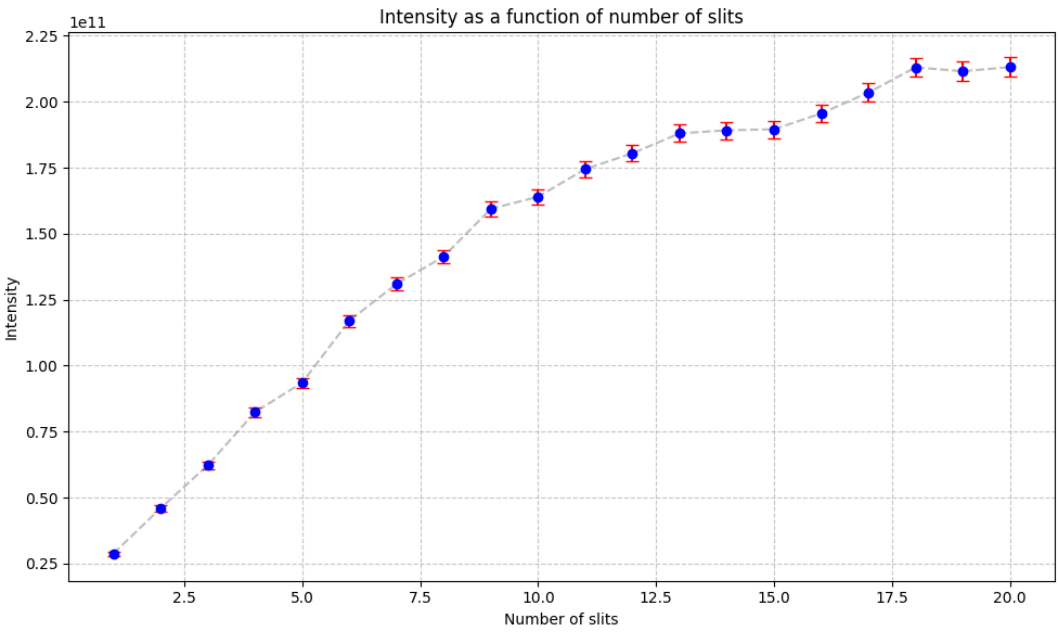

(a) Bender that breaks line of sight once

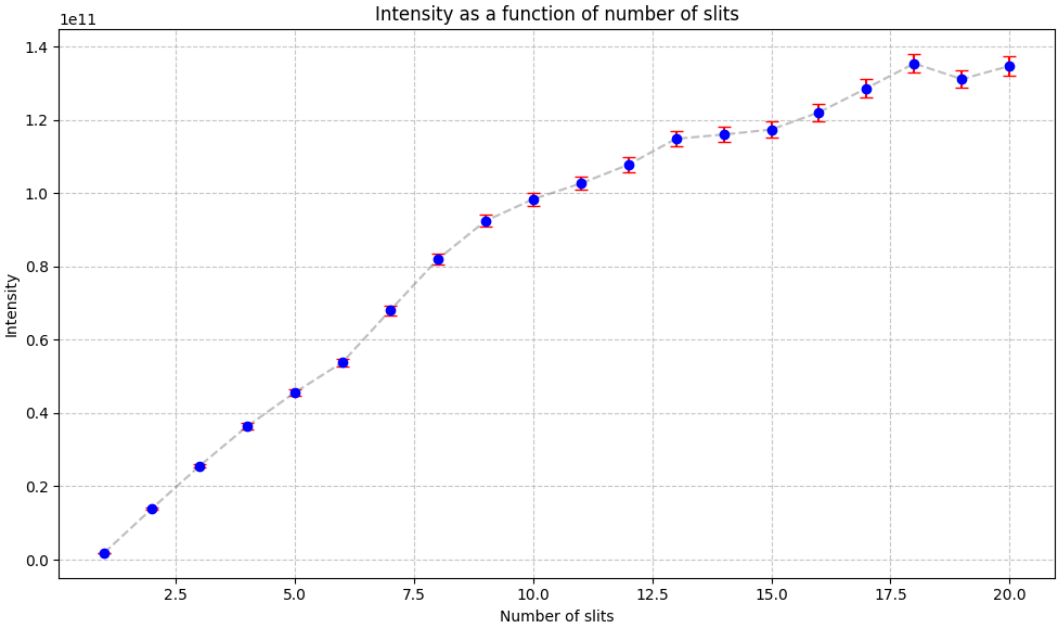

(b) Bender that breaks line of sight twice

Figure 8: Intensity as a function of number of slits, simplified nEDM bender, m-value = 2

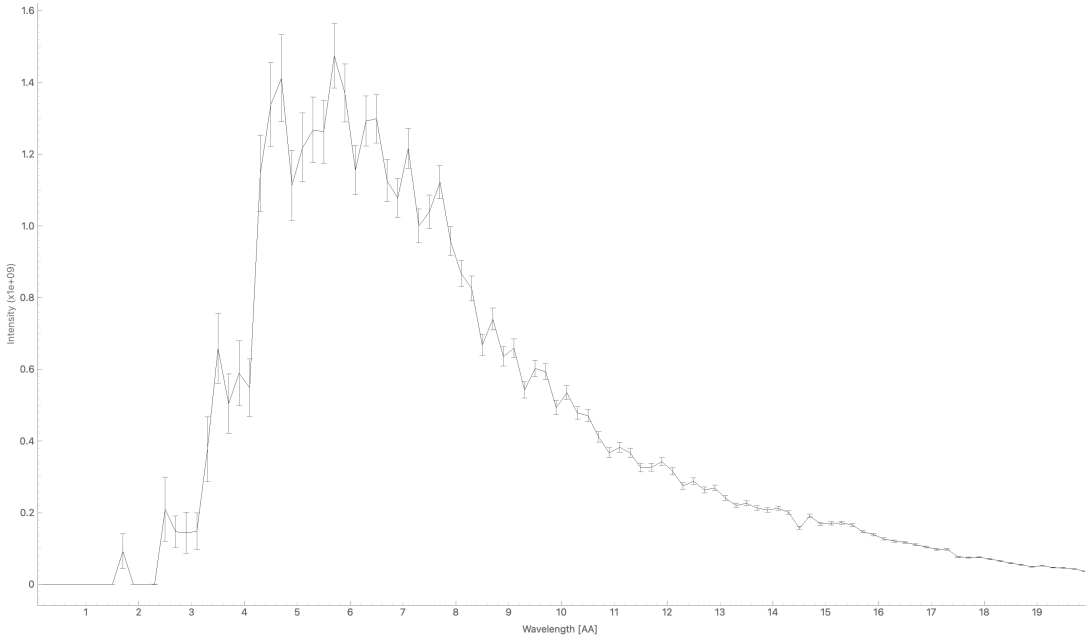

(a) Bender that breaks line of sight once

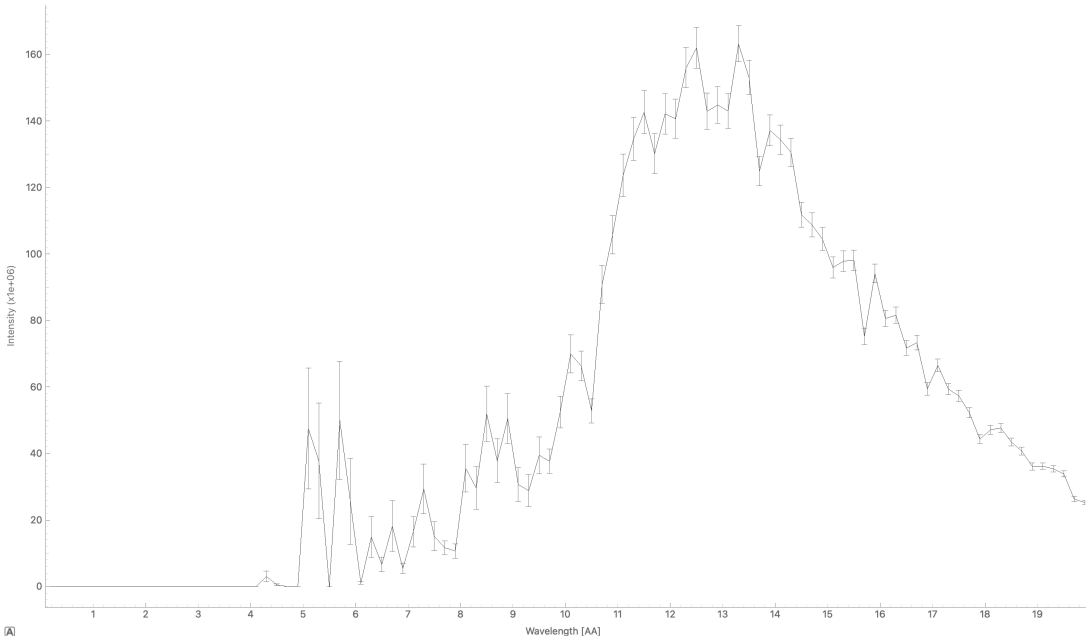

(b) Bender that breaks line of sight twice

Figure 9: Wavelength spectrum after bender, simplified nEDM bender, m-value = 2

Additionally, a smooth vertical bender, with a cross section of $0.1506 \times 0.1446\ m^2$, was placed 60 cm downstream of the monolith guide, with rotation $\theta_x = 0.33°$ and $\theta_y = -0.28°$.

Neutron intensity was simulated for vertical bender guides, shown in Figure 10, with lengths of 11.35 m and 15 m, each tested with m-values 1 and 2. The bend radius was varied to quantify its impact on intensity while ensuring no direct line of sight to the source. A larger bending radius than 71 m for the 11.35 m bender and 176 m for the 15 m bender resulted in a high-energy neutrons appearing in the wavelength plot, which is a clear indication that line of sight was not broken, and thus 71 m and 176 m respectively constitute the upper limits of the plots in Figure 12.

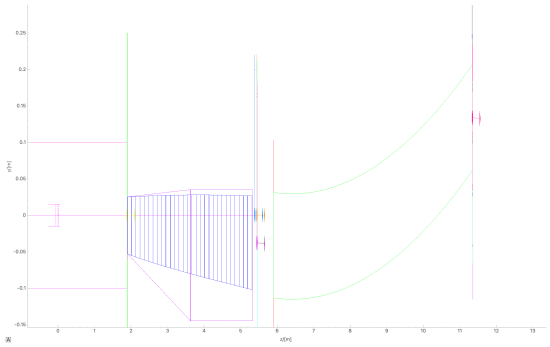

(a) McStas setup: Losing line of sight at 11.35 m

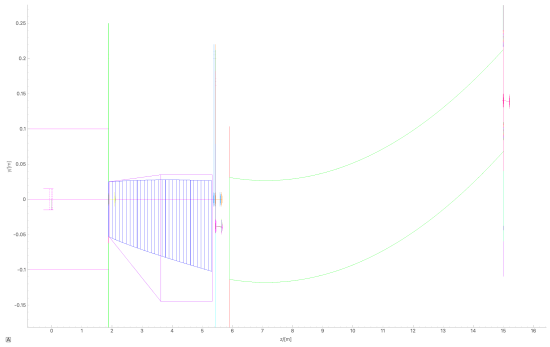

(b) McStas setup: Losing line of sight at 15 m

Figure 10: Vertical bender model

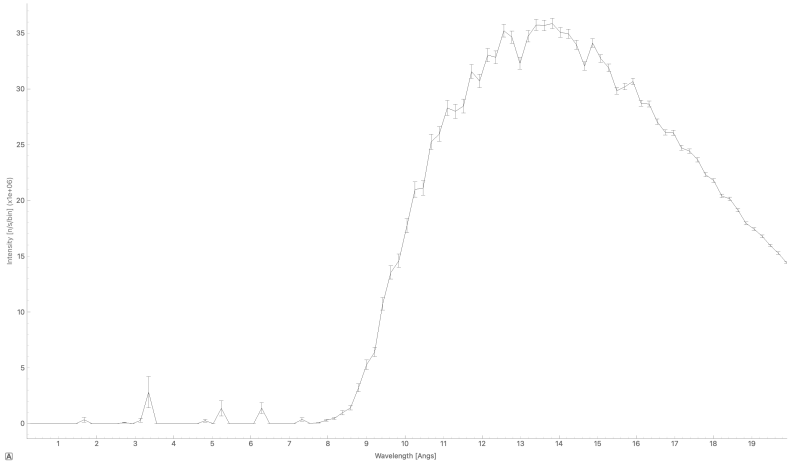

(a) Bending radius 72m

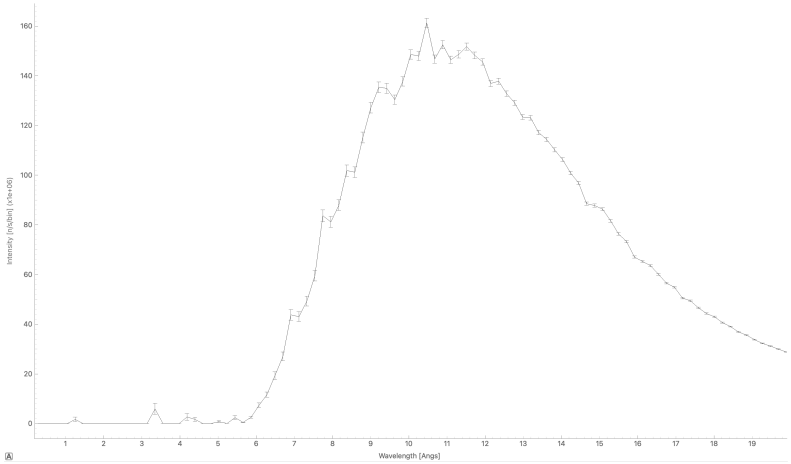

(b) Bending radius 177m

Figure 11: Wavelength plot for guides that don't break line of sight, m-value = 1

Wavelength distributions right after the benders at 11.35 m (radius 71 m) and 15 m (radius 175 m) are shown in Figure 13. It can be observed that shorter wavelengths are filtered out by all four setups, but to different extents, as presented in Table 1. The threshold for filtered out wavelengths was chosen to be 5 percent of the peak intensity. Intensities, uncertainties, and filtered out wavelengths and corresponding parameters are presented in table 1.

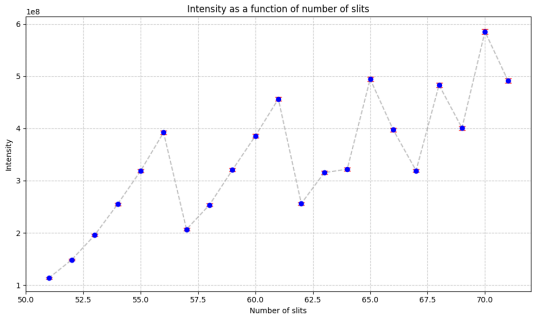

(a) 11.35 m, m-value = 1

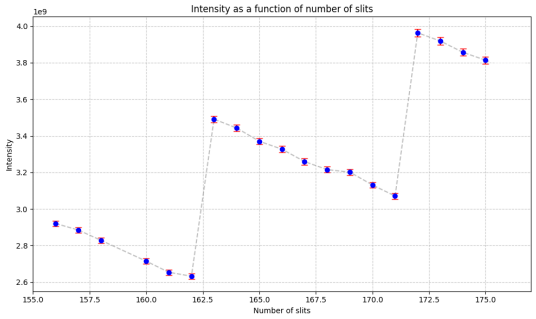

(b) 15 m, m-value = 1

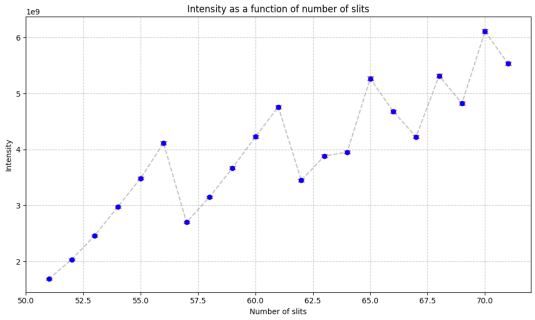

(c) 11.35 m, m-value = 2

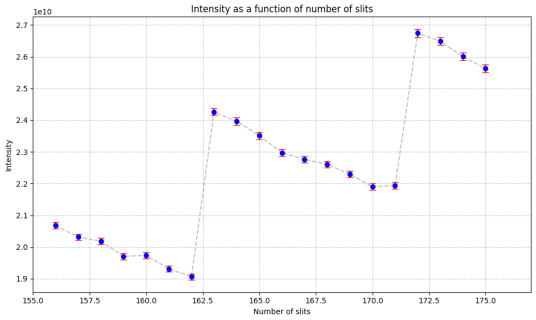

(d) 15 m, m-value = 2

Figure 12: Intensity as a function of bender radius, for 11.35 m and 15 m long benders with m-value 1 and 2

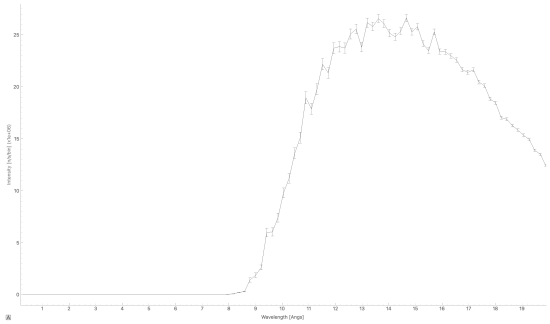

(a) 11.35 m, m-value = 1

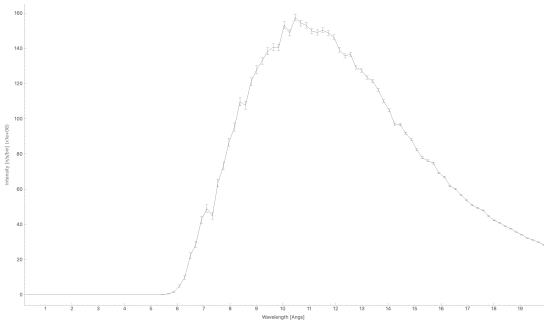

(b) 15 m, m-value = 1

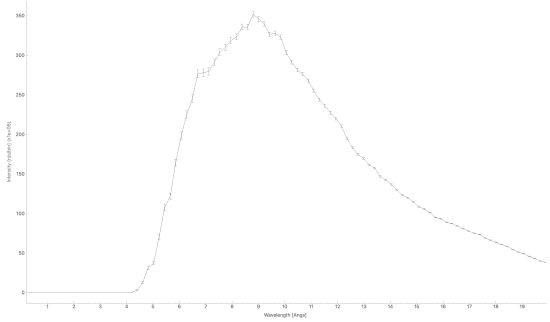

(c) 11.35 m, m-value = 2

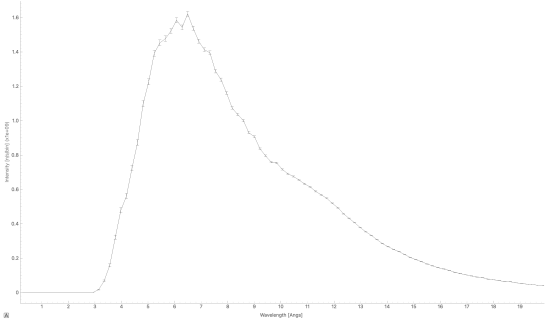

(d) 15 m, m-value = 2

Figure 13: Wavelength plot for guides breaking line of sight at 11.35 m and 15 m, with m-value 1 and 2

Table 1: Intensities, uncertainties, and filtered out wavelengths (below 5% of peak intensity) at bender exit for vertical bender configurations

Guide Endpoint (m)	**m-Value**	**Bend Radius** (m)	**Intensity** (n/s)	**Uncertainty** (n/s)	**Filtered out Wavelengths** (Å)
11.35	1	71	$4.800 \cdot 10^{8}$	$3.980 \cdot 10^{6}$	0 – 7.8
11.35	2	71	$5.499 \cdot 10^{9}$	$3.117 \cdot 10^{7}$	0 – 4.4
15	1	175	$3.923 \cdot 10^{9}$	$1.983 \cdot 10^{7}$	0 – 5.7
15	2	175	$2.632 \cdot 10^{10}$	$1.223 \cdot 10^{8}$	0 – 3.1

3 Discussion

The simulations performed during this internship gave a clearer picture of how guide geometry and bender configurations influence neutron intensity in the target region. Angular adjustments showed that small rotations around the x- and y-axes can noticeably affect flux, and a moderate widening of the guide exit led to further improvement.

Changing the supermirror m-value illustrated the balance between achievable intensity and component complexity. Both simplified nEDM-type benders and vertical benders that block line of sight were found to alter the wavelength spectrum, though with some reduction in flux. With a bender that ends at 11.35 m with a radius of 71 m, the intensity is 3 orders of magnitude lower than what you get with a straight guide that ends at 15 m. The number of slits and the bend radius also turned out to be important factors. The intensity plots also shines light on another unknown, the cause of the periodical fluctuations that can be seen best in Figure 12, but this require further investigation.

Altogether, the results provide practical guidance for designing neutron guides, showing how different bender types lead to characteristic spectra and intensities, which can inform further work on the HIBEAM beamline at ESS